4466 *Inorg. Chem.* **2010**, *49*, 4466–4470
DOI: 10.1021/ic902047f

Inorganic Chemistry
Article

Solvent Effects on Isomerization in a Ruthenium Sulfoxide Complex

Tod A. Grusenmeyer,[†] Beth Anne McClure,[†] Christopher J. Ziegler,[‡] and Jeffrey J. Rack*[,†]

[†]*Department of Chemistry and Biochemistry, Nanoscale and Quantum Phenomena Institute, Ohio University, Athens, Ohio 45701, and* [‡]*Department of Chemistry, Knight Chemical Laboratory, University of Akron, Akron, Ohio 44325*

Received October 15, 2009

We report the structure, electrochemistry, and isomerization kinetics for [Ru(bpy)(biq)(OSO)](PF_6), where bpy is 2,2′-bipyridine, biq is 2,2′-biquinoline, and OSO is 2-methylsulfinylbenzoate. UV−visible and infrared data are suggestive of intramolecular S→O and O→S isomerization of the sulfoxide. Cyclic voltammetry reveals evidence for isomerization triggered by oxidation and reduction. Of particular note is the variation of the S→O isomerization rate constant in different solvents. The rates were found to be 3.2 (±0.4) s^{-1} in propylene carbonate, 0.80 (±0.03) s^{-1} in acetonitrile, and 0.26 (±0.01) s^{-1} in dichloromethane.

Introduction

Electron transfer induced conformational changes are central to the operation of molecular machines and other types of molecular bistability.[1−4] A number of studies have revealed that reduction or oxidation of interlocked rotaxanes results in translocation of a molecular unit from one site to another.[5−7] However, certain transition metal complexes exhibit bistability through isomerization of bound ambidentate ligands.[8,9] For example, pentaammine ruthenium complexes of dimethylsulfoxide (dmso) undergo intramolecular linkage isomerization (S vs O) following oxidation and reduction of ruthenium.[10−13] Recently, we have developed a class of simultaneously photochromic and electrochromic polypyridine ruthenium sulfoxide complexes based on S→O and O→S isomerization.[14−18] In our studies, we have found an unusual solvent dependence on the intramolecular S→O isomerization rate.

Experimental Section

Materials. The ruthenium starting material [(*p*-cym)-Ru(bpy)Cl]Cl, where *p*-cym is *para*-cymene and bpy is 2,2′-bipyridine, was synthesized according to a modified procedure for the complex [(Bz)Ru(bpy)Cl]Cl by starting from [(*p*-cym)$RuCl_2]_2$ instead of [(Bz)$RuCl_2]_2$.[19,20] The synthesis of the ligand OSO has been described previously.[14] The reagents 2,2′-bipyridine (bpy), 2,2′-biquinoline ligand (biq), 2-methylthiobenzoic acid (OS), lithium chloride, and 3-chloroperoxybenzoic acid (*m*CPBA) were purchased from Sigma Aldrich and used as received. Silver hexafluorophosphate ($AgPF_6$) and silver trifluoromethanesulfonate (AgOTf) were purchased from Strem and used as received. Tetra *n*-butyl ammonium hexafluorophosphate ($TBAPF_6$) was purchased from Fluka and recrystallized from hot ethanol three times before use. The solvents *N*,*N*-dimethylformamide (DMF), ethanol, diethyl ether, acetone, triethylamine, 1,2-dichloroethane, dichloromethane, and methanol were purchased from VWR and used without further purification. Acetonitrile and dichloromethane for electrochemical experiments were of spectroscopic grade and purchased from Burdick and Jackson. Anhydrous propylene carbonate used for electrochemical experiments was purchased from Sigma Aldrich and used without further purification. Deuterated solvents (d^6-dmso, d^2-D_2O, and

*To whom correspondence should be addressed. E-mail: rackj@ohio.edu.

(1) Silvi, S.; Venturi, M.; Credi, A. *J. Mater. Chem.* **2009**, *19*, 2279–2294.
(2) Rescifina, A.; Zagni, C.; Iannazzo, D.; Merino, P. *Curr. Org. Chem.* **2009**, *13*, 448–481.
(3) Bonnet, S.; Collin, J. P.; Koizumi, M.; Mobian, P.; Sauvage, J. P. *Adv. Mater.* **2006**, *18*, 1239–1250.
(4) Stoddart, J. F. *Chem. Soc. Rev.* **2009**, *38*, 1802–1820.
(5) McNitt, K. A.; Parimal, K.; Share, A. I.; Fahrenbach, A. C.; Witlicki, E. H.; Pink, M.; Bediako, D. K.; Plaisier, C. L.; Le, N.; Heeringa, L. P.; Vander Griend, D. A.; Flood, A. H. *J. Am. Chem. Soc.* **2009**, *131*, 1305–1313.
(6) Spruell, J. M.; Paxton, W. F.; Olsen, J. C.; Benitez, D.; Tkatchouk, E.; Stern, C. L.; Trabolsi, A.; Friedman, D. C.; Goddard, W. A.; Stoddart, J. F. *J. Am. Chem. Soc.* **2009**, *131*, 11571–11580.
(7) Periyasamy, G.; Sour, A.; Collin, J.-P.; Sauvage, J.-P.; Remacle, F. *J. Phys. Chem. B.* **2009**, *113*, 6219–6229.
(8) Hamaguchi, T.; Inoue, Y.; Ujimoto, K.; Ando, I. *Polyhedron* **2008**, *27*, 2031–2034.
(9) Johansson, O.; Johannissen, L. O.; Lomoth, R. *Chem.—Eur. J.* **2009**, *15*, 1195–1204.
(10) Smith, M. K.; Gibson, J. A.; Young, C. G.; Broomhead, J. A.; Junk, P. C.; Keene, F. R. *Eur. J. Inorg. Chem.* **2000**, 1365–1370.
(11) Yeh, A.; Scott, N.; Taube, H. *Inorg. Chem.* **1982**, *21*, 2542–2545.
(12) Sano, M. *Struct. Bonding* (*Berlin*) **2001**, *99*, 117–139.
(13) Sano, M.; Taube, H. *Inorg. Chem.* **1994**, *33*, 705–709.
(14) McClure, B. A.; Mockus, N. V.; Butcher, J., D. P.; Lutterman, D. A.; Turro, C.; Petersen, J. L.; Rack, J. J. *Inorg. Chem.* **2009**, *48*, 8084–8091.
(15) Rack, J. J. *Z. Kristallogr.* **2008**, *223*, 356–362.
(16) Rack, J. J. *Coord. Chem. Rev.* **2009**, *253*, 78–85.
(17) McClure, B. A.; Rack, J. J. *Angew. Chem., Int. Ed.* **2009**, *48*, 8556–8558.
(18) McClure, B. A.; Abrams, E. R.; Rack, J. J. *J. Am. Chem. Soc.* **2010**, *132*, 5428–5436.
(19) Bennett, M. A.; Smith, A. K. *Dalton Trans.* **1974**, 233–241.
(20) Freedman, D. A.; Evju, J. K.; Pomije, M. K.; Mann, K. R. *Inorg. Chem.* **2001**, *40*, 5711–5715.

Published on Web 04/22/2010
© 2010 American Chemical Society

d^4-CD_3OD) were obtained from Cambridge Isotope Laboratories and used as received.

[Ru(bpy)(biq)Cl$_2$]. This complex was obtained by an altered synthesis from that described by Heijden et al.[21] Orange [(*p*-cym)-Ru(bpy)Cl]Cl (502 mg, 1.09 mmol), 2,2′-biquinoline (284 mg, 1.10 mmol), and 8 equiv of LiCl (312 mg, 7.35 mmol) were added to 2 mL of DMF. The reaction was stirred at reflux for 2.5 h under nitrogen. The solution was allowed to cool to room temperature and added to 50 mL of acetone. The dark green product was isolated by vacuum filtration, rinsed with 15 mL of water, washed with ether (3 × 15 mL), and air-dried. Yield: 502 mg (74.6%). UV−vis (MeOH) λ_{max} = 590 nm (ε_{590} = 6140 M^{-1} cm^{-1}), ^{1}H NMR (d^6-dmso, 300 MHz): δ 9.73 (t, 2 H), 8.71 (q, 2 H), 8.59 (d, 1 H), 8.55 (d, 1 H), 8.44 (d, 1 H), 8.25 (d, 1 H), 8.16 (d, 1 H), 8.07 (t, 1 H), 7.88 (d, 1 H), 7.73 (m, 4 H), 7.51 (d, 1 H), 7.42 (t, 1 H), 7.06 (t, 2 H), 6.95 (d, 1 H). Characterization by ^{1}H NMR agrees with previously published results.

[Ru(bpy)(biq)(OH$_2$)$_2$](OTf)$_2$·0.5CH$_2$Cl$_2$·2H$_2$O. Dark green [Ru(bpy)(biq)Cl$_2$] (52.2 mg, 0.0893 mmol) was dissolved in 10 mL of water and purged with argon for 10 min. Two equivalents of silver triflate (AgOTf) (51.5 mg, 0.200 mmol) were added, and the reaction mixture was stirred under reflux and argon for 4 h. The solution turned a deep purple as the reaction progressed during which time solid AgCl precipitated. The solution was cooled to 0 °C overnight to ensure complete precipitation of AgCl. The solution was filtered to collect 2 equiv of AgCl and rinsed with water until the filtrate was colorless. The filtrate solution was concentrated to approximately 1 mL via rotary evaporation to which dichloromethane was added dropwise to induce precipitation. The solution was cooled in an ice bath for an hour before isolation by vacuum filtration. The solid was rinsed with cold dichloromethane (2 × 5 mL) and diethyl ether (2 × 5 mL) and air-dried. The solid was further dried overnight under vacuum at room temperature. The ^{1}H NMR spectrum reveals 0.5 equiv of CH_2Cl_2. Yield: 58.5 mg (70.3%). UV−vis: (H_2O) λ_{max} = 556 nm (8900 M^{-1} cm^{-1}), 435 nm (shoulder, 2890 M^{-1} cm^{-1}). ^{1}H NMR (D_2O, 300 MHz): δ 8.89 (d, 1 H), 8.72 (m, 3 H), 8.54 (m, 2 H), 8.27−8.35 (m, 4 H), 7.77−7.90 (m, 5 H), 7.75 (t, 1 H), 7.40 (t, 1 H), 7.11 (t, 1 H), 6.97 (t, 1 H), 6.39 (d, 1 H), 5.42 (s, 2 H, 0.5 CH_2Cl$_2$) ppm. Elemental Analysis: Calculated for [Ru($C_{10}H_8N_2$)($C_{18}H_{12}N_2$)(OH_2)$_2$]-(OTf)$_2$·0.5CH_2Cl_2·2 H_2O: C, 39.96%; H, 3.11%; N, 6.02%. Found: C, 39.69%; H, 2.79%; N, 6.01%.

[Ru(bpy)(biq)(OSO)](PF$_6$)·0.5H$_2$O. Dark green [Ru(bpy)-(biq)Cl$_2$] (158 mg, 0.255 mmol) was allowed to react with 2-methylsulfinylbenzoic acid (OSO) (51.7 mg, 0.281 mmol), an excess of triethylamine (75 μL), and 2 equiv of $AgPF_6$ (145 mg, 0.572 mmol) in 40 mL of ethanol. The reaction was brought to reflux for 4.5 h under nitrogen. The solution changed from green to deep red as the reaction progressed during which time solid AgCl precipitated. The solution was cooled to −30 °C to ensure complete precipitation of AgCl and was then filtered to collect 2 equiv of AgCl. The solvent was removed from the filtrate by rotary evaporation. The resulting residue was dissolved in 50 mL of dichloromethane and 2 mL of acetonitrile. The solution was extracted with 15 mL (2 × 7.5 mL) of an aqueous solution of LiOH·H_2O (13 mg). The organic layer was dried with anhydrous magnesium sulfate, and the solvent was removed by rotary evaporation. Approximately 2 mL of ethanol was added to the residue, and 5 mL of diethyl ether was added to complete precipitation. The solid was isolated via vacuum filtration, washed with diethyl ether (2 × 15 mL), and air-dried. Yield: 186 mg (84.8%). UV−vis: (MeOH) λ_{max} = 465 nm (S-bonded, ε_{465} = 3490 M^{-1} cm^{-1}), 572 nm (O-bonded, ε_{572} = 6410 M^{-1} cm^{-1}). ν(S=O) = 1101 cm^{-1} (S-bonded), 1006 cm^{-1} (O-bonded). ^{1}H NMR (d^4-CD_3OD, 500 MHz): δ 9.02 (d, 1 H), 8.89 (d, 1 H), 8.83 (d, 1 H), 8.81 (s, 2 H), 8.75 (d, 1 H), 8.71 (d, 1 H), 8.68 (d, 1 H), 8.51 (d, 1 H), 8.47 (t, 1 H), 8.26 (t, 1 H), 8.12 (d, 1 H), 7.85 (d, 1 H), 7.78 (t, 1 H), 7.73 (t, 1 H), 7.66 (t, 1 H), 7.59 (t, 1 H), 7.49 (t, 1 H), 7.48 (t, 1 H), 7.32 (d, 1 H), 7.20 (t, 1 H), 7.09 (m, 2 H), 6.27 (d, 1 H), 2.04 (s, 3 H). Elemental Analysis: Calculated for [Ru($C_{10}H_8N_2$)($C_{18}H_{12}N_2$)($C_8H_7O_3S$)]PF_6·0.5H_2O: C, 50.82%; H, 3.32%; O, 6.58%; N, 6.59% S, 3.77%. Found: C, 50.84%; H, 3.25%; O, 6.53%; N, 6.71%; S, 3.96%.

Instrumentation. Cyclic voltammetry was performed on a CH Instruments CH1730A Electrochemical Analyzer. This workstation contains a digital simulation package as part of the software package to operate the workstation (CHI version 2.06). The working electrode was a glassy-carbon electrode (1.5 mm, BASi), the counter electrode was a Pt wire, and the reference electrode was a Ag/$AgPF_6$ electrode. Electrochemical measurements were performed in acetonitrile, dichloromethane, and propylene carbonate solutions containing 0.1 M $TBAPF_6$ electrolyte in a one compartment cell. Electronic absorption spectra were collected on an Agilent 8453 spectrophotometer. Bulk photolysis experiments were conducted using a 100 W xenon-arc lamp (Oriel) fitted with a Canon standard camera UV filter. Infrared spectra were obtained on a Nicolet 380 FT-IR spectrometer by evaporating 1,2-dichloroethane solutions onto 25 mm × 4 mm KBr plates. Proton nuclear magnetic resonance (^{1}H NMR) spectra were recorded on either a 300 MHz Bruker AG or a 500 MHz Varian INOVA500 spectrometer in deuterated dmso, water, and methanol (d^6- dmso, d^2-D_2O, d^4-CD_3OD).

Electrochemistry. Rates of electrochemically induced isomerization were obtained by variation of the scan rate in cyclic voltammetry from approximately 0.1−3 V s^{-1}. The rate constant k was found by determining the slope of the left side of eq 1 plotted as a function of inverse scan rate (ν^{-1}). In eq 1 E_p is the S-bonded anodic peak potential, $E_{1/2}$ is the average between the S-bonded anodic and cathodic peak potentials, F is Faraday's constant, T is temperature and was 300 K, n is the number of electrons transferred (n = 1). Equation 1 was derived from eq 2 for an irreversible chemical process following a reversible electron transfer event as described by Nicholson and Shain.[22] Equation 2 has been modified so that the second term is positive rather than negative to account for the isomerization reaction following oxidation rather than reduction as described by Delahay.[23,24]

$$e^{1.560}e^{2nF/RT(E_{1/2}-E_p)} = \frac{kRT}{nF}\left(\frac{1}{\nu}\right) \quad (1)$$

$$E_p = E_{1/2} + \frac{RT}{nF}\left(0.780 - \ln\sqrt{\frac{kRT}{nF\nu}}\right) \quad (2)$$

Crystallography. Crystals suitable for structural determination were obtained by slow addition of diethyl ether to a saturated acetonitrile solution. Single crystal X-ray diffraction data were collected at 100 K (Bruker KRYO-FLEX) on a Bruker SMART APEX CCD-based X-ray diffractometer system equipped with a Mo-target X-ray tube (λ = 0.71073 Å). The detector was placed at a distance of 5.009 cm from the crystal. Crystals were placed in paratone oil upon removal from the mother liquor and mounted on a plastic loop in the oil. Integration and refinement of crystal data were done using Bruker SAINT software package and Bruker SHELXTL (version 6.1) software package, respectively.[25] Absorption correction was completed by using the SADABS program.

(21) Heijden, M.; van Vliet, P. M.; Haasnoot, J. G.; Reedijk, J. *Dalton Trans.* **1993**, 3675–3679.

(22) Nicholson, R. S.; Shain, I. *Anal. Chem.* **1964**, *36*, 706–723.

(23) Delahay, P. *J. Am. Chem. Soc.* **1953**, *75*, 1190–1196.

(24) Delahay, P. *New Instrumental Methods in Electrochemisty*; Interscience: New York, 1954.

(25) Sheldrick, G. M. *SHELXTL, Crystallographic Software Package*, Version 6.10; Bruker-AXS: Madison, WI, 2000.

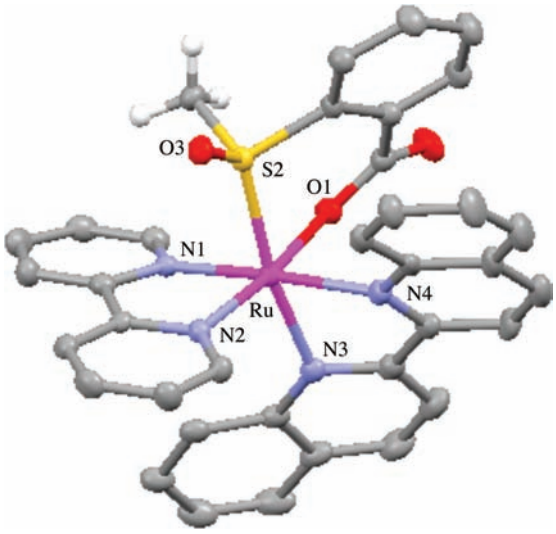

Figure 1. Molecular structure of $[Ru(bpy)(biq)(OSO)](PF_6)\cdot 2CH_3CN$. Thermal ellipsoids have been rendered at 50% probability. Anion, solvent, and certain hydrogen atoms have been omitted for clarity. Selected metrical parameters: Ru−S 2.2304(8) Å; S−O 1.479(2) Å; O−S−Ru 122.04°.

Results and Discussion

The tris-heteroleptic ruthenium complex, $[Ru(bpy)(biq)(OSO)]^+$, where bpy is 2,2′-bipyridine, biq is 2,2′-biquinoline, and OSO is 2-methylsulfinylbenzoate, is prepared following modification to the general procedure originally described by Freedman and Mann.[19,20] This complex is simply prepared by reaction of bipyridine with the ruthenium cymene dichloride dimer to yield [Ru(bpy)(*p*-cym)Cl]Cl, where *p*-cym is *para*-cymene. Subsequent reaction of this monomer with biquinoline yields $[Ru(bpy)(biq)Cl_2]$, which is then allowed to react with 2-methylsulfinylbenzoic acid in the presence of NEt_3 and $AgPF_6$ to yield $[Ru(bpy)(biq)(OSO)](PF_6)$. Alternately, the biquinoline ligand may be added to the ruthenium cymene dimer prior to the addition of bipyridine.[26] In our experience, the OSO ligand must be added last. We surmise that the monoanionic nature of the OSO ligand makes isolation and handling of the intermediary complexes difficult.

Shown in Figure 1 is the molecular structure of $[Ru(bpy)(biq)(OSO)]^+$ with crystallographic data presented in Table 1. The complex crystallizes in space group $P2_12_12_1$, and the complex is clearly chiral. The biquinoline displays a pronounced saddling, and its bulk leads to a distorted octahedral geometry about ruthenium. The angles formed by the chelates are 79.2° (bipyridine, N1−Ru1−N2), 77.6° (biquinoline, N3−Ru1−N4), and 84.5° (OSO, O1−Ru1−S2). Curiously, despite the bulk of the biquinoline ligand, the benzoate ring of OSO is oriented *toward* the outer ring of the biquinoline ligand. Indeed, the centroid-to-centroid distance between these two rings is 3.69 Å, suggestive of an intramolecular $\pi-\pi$ stacking interaction. Of particular note is the Ru−S bond distance of 2.2304(8) Å and the S−O bond distance of 1.479(2) Å. For comparison, closely related $[Ru(bpy)_2(OSO)]^+$ features Ru−S and S−O bond distances of 2.213(1) and 1.479(2) Å, respectively.[27] The $Ru-O_{benzoate}$ bonds are identical, 2.085(2) and 2.086(2) Å, for the biquinoline and bipyiridine complexes, respectively. There are only a few crystallographic reports of ruthenium biquinoline structures.[26,28−30] These structures feature substantial buckling or a "banana-shaped curvature" of the biquinoline chelate.[30] For example, the torsion angle defined by N3−C19−C20−N4 in $[Ru(bpy)(biq)(OSO)]^+$ is −4.5° which is similar to −8.6° observed in $[Ru(tpy)(biq)Cl]^+$, where tpy is 2,2′:6′,2″-terpyridine. The reported structure of $[Ru(p\text{-cym})(biq)Cl_2]$ is of poor quality so that it does not allow possible extraction of this metric for comparison.[26] Elemental analyses and ^1H NMR spectra of the sample are consistent with the crystal structure.

Table 1. Crystal Data for $[Ru(bpy)(biq)(OSO)](PF_6)\cdot 2CH_3CN$

formula weight	923.82
temperature, K	100(2)
wavelength, Å	0.71073
crystal	orthorhombic
space group	$P2(1)2(1)2(1)$
unit cell dimensions, Å, deg	$a = 7.9092(13)$, $\alpha = 90$
	$b = 17.075(3)$, $\beta = 90$
	$c = 28.341(5)$, $\gamma = 90$
volume, $Å^3$	3827.5(11)
Z	4
density (calculated), Mg/m^3	1.603
absorption coefficient, mm^{-1}	0.584
$F(000)$	1872
crystal size, mm^3	0.35 × 0.08 × 0.07
θ range for data collection	1.39 to 27.50°
index ranges	$-10 \le h \le 10$
	$-22 \le k \le 2$
	$-36 \le l \le 36$
reflections collected	31898
independent reflections	8678 [R(int) = 0.0547]
completeness to θ = 27.50°	99.5%
absorption correction	SADABS
max. and min transmission	0.9603 and 0.8217
refinement method	full-matrix least-squares on F^2
Data/restraints/parameters	8678/0/526
Goodness-of-fit on F^2	0.954
Final R indices [I > 2sigma(I)]	R1 = 0.0320, wR2 = 0.0638
R indices (all data)	R1 = 0.0402, wR2 = 0.0741
absolute structure parameter	0.00(2)
largest diff. peak and hole	0.459 and −0.570 e $Å^{-3}$

The visible spectrum of *S*-$[Ru(bpy)(biq)(OSO)]^+$ in propylene carbonate features a broad, low energy absorption at 474 nm ($\varepsilon = 3240 \pm 10$ M^{-1} cm^{-1}; orange trace; Figure 2), which is appropriately shifted to the red in comparison to $[Ru(bpy)_2(OSO)]^+$ (λ_{max} = 396 in methanol).[14,27] This absorption is ascribed to a metal-to-ligand charge-transfer (MLCT) transition based on its intensity and energy. Consistent with other photochromic ruthenium polypyridine sulfoxide complexes, charge-transfer excitation results in the formation of a new absorption at 572 nm ($\varepsilon = 5260 \pm 140$ M^{-1} cm^{-1}; purple trace; Figure 2). For comparison, $[Ru(bpy)(biq)(OH_2)_2]^{2+}$ exhibits λ_{max} at 435 and 556 nm in aqueous solution. This is significant as the inner coordination sphere contains two O-bonded ligands on the $[Ru(bpy)(biq)]^{2+}$ fragment. The absorption results are indicative of intramolecular S→O isomerization.

Structural evidence in support of isomerization comes from infrared spectroscopy (Figure 3). The black trace shows the ground state S-bonded complex which features ν(S═O) at

(26) Lalrempuia, R.; Kollipara, M. R. *Polyhedron* **2003**, *22*, 3155–3160.
(27) Butcher, J., D. P.; Rachford, A. A.; Petersen, J. L.; Rack, J. J. *Inorg. Chem.* **2006**, *45*, 9178–9180.
(28) Gut, D.; Rudi, A.; Kopilov, J.; Goldberg, I.; Kol, M. *J. Am. Chem. Soc.* **2002**, *124*, 5449–5456.
(29) Youssef, A. O.; Khalil, M. M. H.; Ramadan, R. M.; Soliman, A. A. *Trans. Met. Chem.* **2003**, *28*, 331–335.
(30) Spek, A. L.; Gerli, A.; Reedijk, J. *Acta Crystallogr., Sect. C* **1994**, *50*, 394–397.

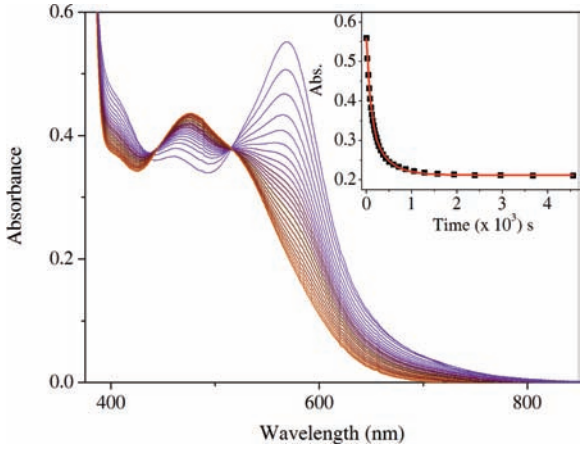

Figure 2. UV−visible spectra of S-bonded (orange) and O-bonded (purple) isomers of $[Ru(bpy)(biq)(OSO)]^+$ in propylene carbonate at 40 °C. Intermediate traces show thermal reversion from O- to S-$[Ru(bpy)(biq)(OSO)]^+$. Inset: kinetic trace (data black squares) at 585 nm with biexponential fit (red line).

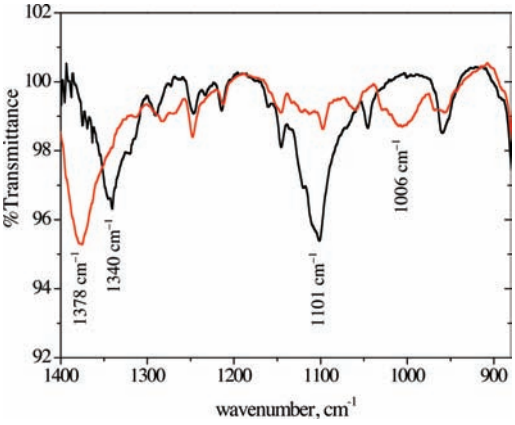

Figure 3. Infrared spectra of S- (black) and O-$[Ru(bpy)(biq)(OSO)](PF_6)$ (red). Spectra are obtained from 1,2-dichloroethane solutions (non-irradiated and irradiated) on KBr disks.

1101 cm^{-1}, in accord with an S-bonded sulfoxide.[31−33] This spectrum is obtained following evaporation of a 1,2-dichloroethane solution containing the ruthenium complex onto a KBr plate. The red trace is obtained following evaporation of an irradiated 1,2-dichloroethane solution containing the ruthenium complex onto a KBr plate. The concentration of the two solutions is similar. The absorption spectrum of the irradiated solution is consistent with full conversion to the O-bonded isomer. The red trace shows a disappearance of the band at 1101 cm^{-1} concomitant with the appearance of a broad feature at 1006 cm^{-1}, consistent with an O-bonded sulfoxide.[31−33] For comparison, $[RuCl_2(dmso)_4]$ features ν(S═O) at 1120 cm^{-1} and 1090 cm^{-1} for three S-bonded dmso ligands and ν(S═O) at 915 cm^{-1} for a single O-bonded dmso ligand. The typical range for O-bonded sulfoxides is ~850 to~1000 cm^{-1}.[32] Interestingly, there are three crystallographically characterized complexes that display a bridging S,O bidentate sulfoxide between two ruthenium(II) cations. For this unusual bonding mode, ν(S═O) is 1017, 1010, and

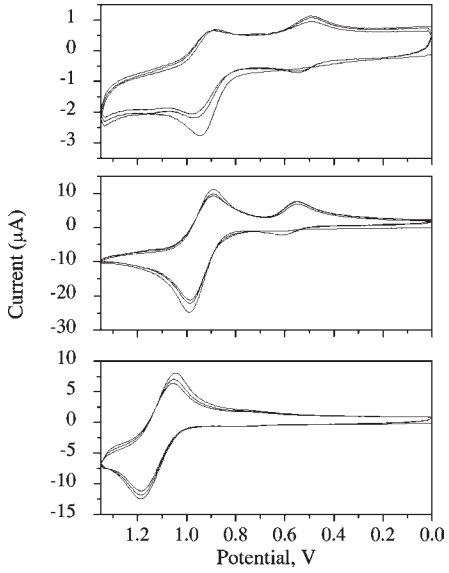

Figure 4. Cyclic voltammograms of $[Ru(bpy)(biq)(OSO)]^+$ in propylene carbonate (top), acetonitrile (middle), and dichloromethane (bottom). Working electrode: glassy carbon; Counter electrode: platinum; Reference electrode: $Ag/AgPF_6$ in CH_3CN; scan rate: 0.2 V/s.

1004 cm^{-1}, respectively for the three reports.[34−36] These values are suspiciously close to that reported for $[Ru(bpy)(biq)(OSO]^+$ and suggest that the metastable state is more accurately characterized as an η^2- or an asymmetric η^2-sulfoxide ligand. Also present in the IR spectra is a demonstrable shift in the 1378 cm^{-1} feature to 1340 cm^{-1}. We tentatively assign this peak to the carboxylate ($RCOO^-$) moiety based on its position and intensity. Such a shift may be expected given the isomerization proposed here. In aggregate, the electronic and infrared spectra permit assignment of the metastable isomer to an O-bonded or η^2-bonded sulfoxide.

Complete reversion of metastable *O*-$[Ru(bpy)(biq)(OSO)]^+$ to ground state *S*-$[Ru(bpy)(biq)(OSO)]^+$ occurs over a period of hours at room temperature in organic solvents (Figure 2, inset). For propylene carbonate, a biexponential decay best fits the absorption versus time data yielding rate constants ($k_{O\rightarrow S}$) of $1.13\,(\pm0.05)\times10^{-2}\,s^{-1}$ and $2.76\,(\pm0.18)\times10^{-3}\,s^{-1}$. In methanol, these rate constants are $1.53\,(\pm0.01)\times10^{-3}\,s^{-1}$ and $1.79\,(\pm0.07)\times10^{-4}\,s^{-1}$. Despite the increased viscosity of propylene carbonate (η = 2.50 mPa·s) relative to methanol (η = 0.59 mPa·s), the reversion rates are faster by a factor of 10 in propylene carbonate than in methanol. These rates are significantly faster than those observed for $[Ru(bpy)_2(OSO)]^+$, where $k_{O\rightarrow S}$ are $9.4(1)\times10^{-4}\,s^{-1}$ and $6.6(1)\times10^{-5}\,s^{-1}$ in propylene carbonate.[14,27] In accord with our previous interpretation of this biexponential behavior, we ascribe the fast rate constant to a relatively small molecular rearrangement prior to the isomerization and the slow rate constant to the isomerization.[14]

Cyclic voltammograms of *S*-$[Ru(bpy)(biq)(OSO)]^+$ are broadly consistent with an electron-transfer triggered isomerization of the bound sulfoxide. First described by Taube[11] and

(31) Alessio, E. *Chem. Rev.* **2004**, *104*, 4203–4242.
(32) Calligaris, M. *Coord. Chem. Rev.* **2004**, *248*, 351–375.
(33) Calligaris, M.; Carugo, O. *Coord. Chem. Rev.* **1996**, *153*, 83–154.
(34) Geremia, S.; Mestroni, S.; Calligaris, M.; Alessio, E. *Dalton Trans.* **1998**, 2447–2448.
(35) Lessing, S. F.; Lotz, S.; Roos, H. M.; van Rooyen, P. H. *Dalton Trans.* **1999**, 1499–1502.
(36) Tanase, T.; Aiko, T.; Yamamoto, Y. *Chem. Commun.* **1996**, 2341–2342.

Table 2. Rate Constants, Solvent, and Reduction Potentials for $[Ru(bpy)_2(OSO)]^+$ and $[Ru(bpy)(biq)(OSO]^+$

	$[Ru(bpy)(biq)(OSO]^+$			$[Ru(bpy)_2(OSO)]^+$		
	PC η = 2.50	CH_3CN η = 0.344	CH_2Cl_2 η = 0.393	PC η_s = 66.14	CH_3CN ε_s = 36.64	CH_2Cl_2 ε_s = 8.93
$k_{S\rightarrow O}$ (s^{-1})	3.2 (±0.4)	0.80 (±0.03)	0.26 (±0.01)	2.01 (±0.4)	1.90 (±0.15)	1.51 (±0.04)
$k_{O\rightarrow S}$ (s^{-1})	1.13×10^{-2} 2.76×10^{-3}	na	na	9.4×10^{-4} 6.6×10^{-5}	na	na
$E_S^{\circ\prime}$ (V)	0.91	0.94	1.12	0.84	0.87	1.06
$E_O^{\circ\prime}$ (V)	0.52	0.58	0.74	0.40	0.50	0.63

later elaborated by Sano,[12,13] S→O and O→S isomerization can be triggered by oxidation of Ru^{II} to Ru^{III} and reduction of Ru^{III} to Ru^{II}, respectively. The S−bonded Ru^{III} sulfoxide is thermodynamically unstable and intramolecularly isomerizes to generate O−bonded Ru^{III}. Similarly, the thermodynamically unstable O-bonded Ru^{II} sulfoxide isomerizes to yield S−bonded Ru^{II}. The driving force for this reaction is the greater covalency of the Ru^{II}−S bond relative to Ru^{II}−O bond.[37] Isomerization rates from these voltammetric scans are typically obtained either through simulation or plots of current ratios versus time. The appearance of the voltammogram is related to the scan rate, the isomerization rate(s), and the switching potential(s).

Shown in Figure 4 are voltammograms of $[Ru(bpy)(biq)(OSO)]^+$ collected in propylene carbonate, acetonitrile, and dichloromethane solutions containing 0.1 M $TBAPF_6$ at a scan rate of 0.2 V/s. As is evident, the appearance of the voltammogram at an identical scan rate and scan range in three different solvents is quite different. In propylene carbonate, upon scanning to positive potentials a one-electron wave is observed, representing oxidation of S-bonded Ru^{II}. Reversing the polarity at the switching potential reveals only a small current wave corresponding to reduction of S-bonded Ru^{III}. A more prominent cathodic wave is observed at less positive potentials, representing reduction of Ru^{III}−O. Reversing the polarity again reveals current waves attributed to both S- and O-bonded $Ru^{3+/2+}$ couples. The O-bonded couple is only formed following oxidation of the S-bonded couple at more positive potentials. The relatively fast isomerization rate results in the small current wave corresponding to reduction of S-bonded Ru^{III}. The voltammogram of the same compound in acetonitrile features more reversible behavior, indicating a slower S→O isomerization rate. In dichloromethane, the couple is nearly reversible pointing to a much slower isomerization rate constant.

Isomerization rate constants ($k_{S\rightarrow O}$) were determined from plots of E_p versus $1/\nu$, where ν is the scan rate (Table 2). The rate constants were found to be 3.2 (±0.4) s^{-1} in propylene carbonate, 0.80 (±0.03) s^{-1} in acetonitrile, and 0.26 (±0.01) s^{-1} in dichloromethane. In comparison to $[Ru(bpy)_2(OSO)]^+$, the rate constants were found to be 2.01 (±0.4) s^{-1} in propylene carbonate, 1.90 (±0.15) s^{-1} in acetonitrile, and 1.51 (±0.04) s^{-1} in dichloromethane. While the same trend is observed, the magnitude of the effect is greatly diminished. Moreover, the S- and O-bonded formal potentials ($E_S^{\circ\prime}$ and $E_O^{\circ\prime}$) follow the same trend for the two complexes. Solvent effects on reaction rates are typically ascribed to static dielectric constant (ε) and viscosity (η) considerations, and these are greatest for propylene carbonate. While both are likely operative here, we favor a more prominent role for viscosity relative to dielectric.[38] This is due in part to recognizing that the dipole moments of the oxidized products, $[Ru^{III}(bpy)(biq)(OSO)]^{2+}$ and $[Ru^{III}(bpy)_2(OSO)]^{2+}$, are not expected to be greatly different, yet the solvent effect is more pronounced for the biquinoline complex. Thus, it appears that the effect reported here is due to a specific solute−solvent interaction involving $[Ru(bpy)(biq)(OSO)]^+$. It is interesting to note that Feringa and co-workers have reported fast isomerization rates in overcrowded alkenes in more viscous solvents relative to less viscous solvents.[39] They advance a hypothesis that the molecule displaces a larger volume in more viscous solvents. Isomerization occurs within a void, and there is less solvent friction acting upon molecular motion. While speculative, a similar effect may be operative in this complex.

In summary, we find that the data presented here are consistent with sulfoxide isomerization in $[Ru(bpy)(biq)(OSO)]^+$. In particular, the infrared spectroscopic data support an O-bonded or η^2-bonded sulfoxide structure for the metastable state. Also, we observe that the S→O and O→S rate constants in $[Ru(bpy)(biq)(OSO)]^+$ vary by more than an order of magnitude depending upon solvent. Future studies will focus on obtaining a more detailed understanding of the role of solvent in these intramolecular isomerizations.

Acknowledgment. We thank Carl P. Myers from Pennsylvania State University and Preston Roeper (OU) for experimental assistance. We acknowledge NSF (CHE 0809699), Ohio University, the Condensed Matter and Surface Science institute and NanoBioTechnology Initiative for funding. T.A.G. recognizes the Provost's Undergraduate Research Fund (PURF) for support of this work. B.A.M. recognizes NDSEG for a graduate fellowship.

Supporting Information Available: Crystallographic Information File (.cif). This material is available free of charge via the Internet at http://pubs.acs.org.

(37) Lutterman, D. A.; Rachford, A. A.; Rack, J. J.; Turro, C. *J. Phys. Chem. A*. **2009**, *113*, 11002–11006.

(38) Attempts to expand the study in more solvents with different dielectric constants, donor properties, and viscosity are not possible because of solubility problems.

(39) Klok, M.; Janssen, L. P. B. M.; Browne, W. R.; Feringa, B. L. *Faraday Discuss*. **2009**, *143*, 319–334.